Quality assessment model of 3 different microkeratomes through confocal microscopy

Jaime Javaloy, MD, PhD, María T. Vidal, MD, Antonio Quinto, OA, Victoria de Rojas, MD, PhD, Jorge L. Alió, MD, PhD

Purpose: To study the quality of the cut created by 3 microkeratomes from 2 different generations using corneal confocal microscopy.

Setting: Department of Refractive Surgery, Instituto Oftalmológico de Alicante, Alicante, Spain.

Methods: Two different studies were conducted: Study 1 and Study 2. Study 1 was a prospective analysis using confocal microscopy examination data from 2 reference groups: Group A (control) with 20 nonoperated eyes of 20 healthy volunteers, and Group B with 50 eyes of 30 patients operated on with the Bausch & Lomb Automated Corneal Shaper (ACS) microkeratome. Study 2 was a prospective randomized double-masked study in which 40 eyes of 20 patients underwent myopic laser in situ keratomileusis by 1 surgeon. The right and left eyes of each patient were randomly and alternatively assigned to Group C, flap made with the Hansatome microkeratome, or Group D, flap made with the Moria M2. Immediately after surgery, the microscopic appearance of the cut was subjectively evaluated by the surgeon. One month postoperatively, flap thickness, particle density, and the subclinical confocal wound healing opacity (WHO) index were evaluated with the corneal confocal microscope.

Results: Surgeon handling comfort was nearly the same with the Hansatome as with the M2 ($P = .540$). However, the apparent quality of the resulting flap was better with the M2 microkeratome ($P = .041$). The depth of the cuts made by the 3 microkeratomes were significantly different ($P<.001$), with the ACS flaps being thinner than the flaps made with the Hansatome or the M2. Particle density at the interface was significantly poorer in the eyes operated on with the ACS, but in these cases the WHO index was significantly greater ($P<.001$ in both cases).

Conclusions: Confocal microscopy is a very useful tool to evaluate the quality of the cut made by different microkeratomes. Overall, the predictability in flap thickness and the apparent quality of the cut made by the Moria M2 microkeratome are better than those obtained with the Hansatome or the ACS. The thin flap made by the ACS microkeratome produced a significantly greater WHO index than the thicker flaps created with the other 2 microkeratomes.

J Cataract Refract Surg 2004; 30:1300–1309 © *2004 ASCRS and ESCRS*

Assessing the quality of corneal refractive surgical procedures and the accompanying technologies is important for health care, economic, and social reasons. Monitoring quality is even more important when procedures and technologies are frequently changing, with the aim of improving outcomes.

Laser in situ keratomileusis (LASIK) is undoubtedly the most frequently used refractive surgery technique for the correction of low to moderate myopia, hyperopia, and astigmatism. Its effectiveness and predictability in producing good unaided visual acuity and its safety in terms of minimal risk of visual acuity loss have been demonstrated.[1] Many variables affect LASIK outcome, such as appropriate patient selection, the sur-

Accepted for publication October 23, 2003.

Reprint requests to Jaime Javaloy Estañ, Instituto Oftalmológico de Alicante, Avda Denia, 111, Alicante, Spain. E-mail: jjavaloy@coma.es.

0886-3350/04/$–see front matter
doi:10.1016/j.jcrs.2003.10.024

geon's experience, and the excimer laser technology that is used. Because microkeratomes are a main source of complications leading to visual loss after LASIK surgery,[2–9] studies that evaluate the reliability and surgical quality of these critical instruments are needed.

The Bausch & Lomb Automatic Corneal Shaper (ACS) has been the most popular microkeratome for many years. Derived from the Automated Lamellar Keratotomy (ALK) system designed by Ruiz,[10] this second-generation automated microkeratome became the model for performance. A number of studies evaluating different aspects of this microkeratome have been conducted.[2,3,11–17] Continued development produced third-generation microkeratomes primarily to satisfy 2 needs: to be able to create a bigger flap for hyperopic ablations and to be able to create a superior hinge. The Hansatome also ushered in this generation and has been widely studied.[2,3,5,11,13,16,18–21]

The Moria M2 microkeratome was designed with a pivoting system over a lateral axis, similar to that of the Hansatome. However, this device has some additional advantages: (1) different suction rings for successive ranges of keratometric values to increase the safety and reliability of flaps made in different types of corneas, and (2) the choice of different meridians for hinge placement.

Up to now, electron microscopy was used to evaluate microkeratome performance.[11,18,22,23] The availability of the confocal microscope, however, has made it possible to study the cornea in vivo and objectively to determine the quality of refractive procedures. In this 2-part study, we attempted to create a quality control standard for objectively comparing the performance of different microkeratomes. Using confocal microscopy (CM), we compared the flaps made by 2 third-generation microkeratomes (Hansatome and Moria M2) with those obtained with a classical second-generation device, the ACS, after LASIK surgery.

Patients and Methods

Study 1: Nonoperated Eyes and ACS-Flap Eyes

We designed 2 different comparison studies: Study 1, eyes that had a flap made with the ACS microkeratome vs. no-surgery eyes, and Study 2, eyes randomly assigned to have a flap made with the Hansatome microkeratome (HT-230, Bausch & Lomb) vs. eyes assigned to have a flap made with the M2 (Moria, Inc.).

The first study was a prospective analysis using data from the CM examinations with 2 reference groups: (1) 20 unoperated healthy control eyes (20 volunteers), and (2) 50 eyes of 30 patients who had surgery with the ACS microkeratome ALK system by 3 different surgeons (J.L.A., J.J., J.R.V.) and analyzed by a different independent investigator (M.T.V.) at the Instituto Oftalmológico de Alicante from September 2000 to March 2001. The desired flap thickness was 160 μm.

The LASIK ablation was performed with the same Technolas 217C excimer laser (PlanoScan, Bausch & Lomb), and the interface in each case was irrigated with 3 mL of balanced salt solution (BSS®) using a bimanual and automated irrigation/aspiration system. Each eye received the same postoperative treatment: tobramycin and dexamethasone (TobraDex®) every 6 hours during week 1 and preservative-free hyaluronic acid 0.1% (Vislube®) every 12 hours during month 1.

All operated eyes were evaluated with a tandem scanning confocal microscope (TSCM; model 165A; ASL) 1 month after surgery. This microscope is equipped with a 24×, 0.6 NA immersion objective. A confocal microscope through focusing (CMTF) analysis was performed to determine the thickness of the corneal flap, to obtain a manual recount of particles found in the interface, and to calculate the wound healing opacity (WHO) index in each case. The use of the confocal microscope is described below. Slitlamp examination was perform to detect any degree of corneal opacity (haze) following U.S. Food and Drug Administration standardized categories: grade 0, clear; grade 1, trace haze; grade 2, mild haze; grade 3, moderate haze; grade 4, marked haze.[24]

Hansatome Flap Eyes vs. M2 Flap Eyes

The second study was a prospective randomized double-masked investigation performed at the same surgical facility. Forty eyes of 20 patients underwent LASIK surgery to correct myopia or myopic astigmatism during March and April 2001. The usual exclusion criteria for photorefractive surgery were applied, and all the patients were informed about their participation in an investigation. The study design followed the terms of the Helsinki's Declaration.[25]

All eyes underwent surgery by one surgeon (J.L.A.), and the data were examined by the same independent investigator (M.T.V.) 1 week and 1 month after the interventions. The surgeon randomly assigned each eye of the patient to 1 of the 2 experimental groups: Group C had the flap made with the Hansatome, and Group D had the flap made with the M2 microkeratome. Both microkeratomes were used with the same cut parameters and with an original new blade. The Hansatome was set for a depth of 160 μm, 9.5 mm flap diameter, and a superior hinge. The M2 was used with the +1 ring (taking the keratometric values of the operated corneas into account), the 8 stop, and the 130 head for a desired cut depth of 160 μm and a superior hinge. The standard speed of pass (2-second pass) was used in all M2 cases. One blade was used in each eye. After making the bilateral

intervention, the surgeon filled out a subjective questionnaire, scoring 0 to 10, from very uncomfortable (0) to very easy to handle (10), for "handling comfort" during the handling of the microkeratome and from 1 to 4 for the apparent quality of the created flap observed under the surgical microscope. Subjective criteria of flap quality included the apparent homogeneity of the flap thickness and the absence of steps, epithelial defects, or any kind of complication induced by the cut. An apparently "perfect" flap received 10 points in the scoring system. At the same time, the surgeon registered the surface measurements (maximum flap diameter and hinge) of the created flap.

The surgical procedure and postoperative care were the same as in the previous Group 1, including use of the Technolas 217C excimer laser, interface irrigation using 3 mL of BSS, TobraDex drops, and Vislube tears. At week 1 and month 1 postoperatively, flap thickness, particle density, and confocal WHO index were evaluated using the corneal confocal microscope. Corneal opacity at the slitlamp was also evaluated on the same postoperative dates.

Confocal Microscopy Evaluations

After instillation of topical anaesthesia (Anestésico Doble), methylcellulose 2.5% (refractive index 1.34) was placed over the probe of the confocal microscope to perform a CMTF analysis. Three main parameters were determined at the central part of the cornea: flap thickness, particle density, and the confocal WHO index. This index indicates the luminous reflectivity from the anterior part of the corneal stroma and is expressed as a nondimensional number equal to the area of the peak of high reflectivity found at the anterior part of the corneal stroma (Figure 1). Though the term *WHO index* has been intended for studying the optical luminous reflectivity in operated corneas, the area of normal high reflectivity peak corresponding to subbasal nervous plexus and normal anterior keratocytes in control eyes has been compared in our study with the profile in operated eyes.

To ensure good reproducibility of the technique and allow direct comparison of scans obtained at different time points, the video camera gain, kilovolts, and black level were kept constant throughout the study. During the examination, at least 3 Z-scans were taken in 2 ways (from epithelium to endothelium and in the reverse) and recorded on Super-VHS videotape. During the CTMF scanning, the focus plane advances to a speed of 64 μm/s. Since the video images are captured and digitalized at 30 frames/second during a continuous scan, consecutive images are separated in the *z*-axis by approximately 2.12 μm (lens speed 160 μm/sec). Each scan was obtained within 10 seconds to obtain 200 to 300 optic frames. The highest quality record was digitalized, and a number between 0 and 1 was given for each luminous intensity belonging to each optic frame. The data were copied in a Microsoft Excel spreadsheet, and a bidimensional graph was created. As illustrated in Figure 1, the horizontal axis

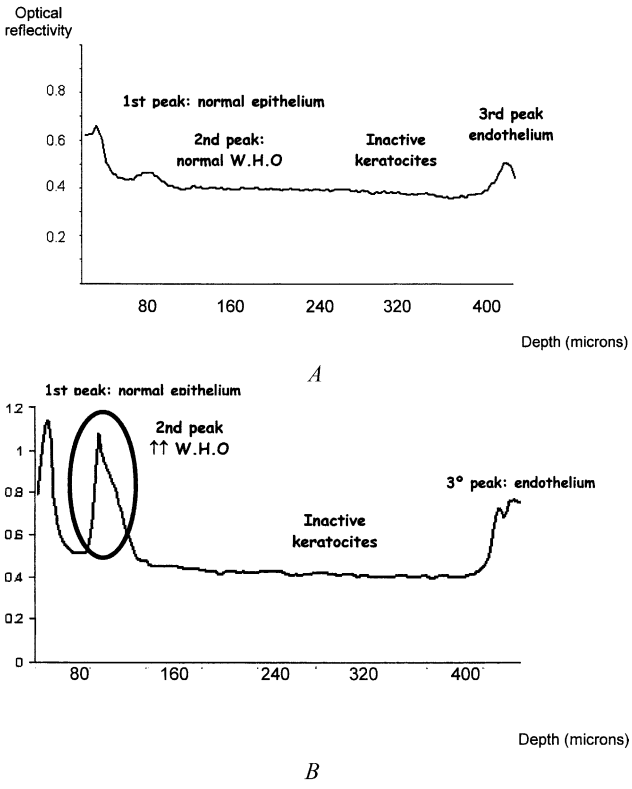

Figure 1. (Javaloy) Example of a CMTF profile in (*A*) a post-LASIK eye with completely clear cornea, and (*B*) a case of LASIK with some degree of subclinical haze (case from another series).

indicated the corneal depth and the vertical indicated the corresponding luminous intensity for each point. In the ordered list of luminous reflectivity (intensity profile), the section corresponding to the peak was identified and the area calculated by adding the rectangular areas belonging to each frame.

Flap thickness was obtained by resetting the micron counter, presented at the TV screen, just when the most superficial image was taken of the epithelial surface. Meanwhile the z-scan was performed as the automatic counter was running, and the depth where the interface was located was determined by observing for the presence of metallic particles on the TV. A small reflectivity peak in the corresponding reflectivity profile could be observed most of the time at this level, permitting the data to be checked. The chosen value in each case was the mean of the 3 double-way z-scans.

To estimate particle density at the interface, the image corresponding to the interface at the central cornea was frozen on the videotape. The image on the TV screen represented a corneal surface with a rectangular shape, which measured 300 μm × 450 μm. Thus, after a manual counting of the number of particles that appeared on the screen, the obtained value was divided by 0.135 to calculate the density of the particles/mm^2. The chosen value for each case was the mean of the three double-way z-scans.

The data were tabulated and analyzed using the statistical package Sigma Stat 2.03 for Windows (Jandel Scientific). When

Table 1. Wound healing opacity index in the study groups.

Parameter	Group A (Control)	Group B (ACS)	Group B (ACS No Haze)	Group B (ACS Subclinical Haze)	Group C (Hansatome)	Group D (M2)
Mean	0.96 ± 0.68	1.39 ± 2.22	0.82 ± 0.85	5.54 ± 4.10	0.44 ± 0.59	0.39 ± 0.31
Range	0.01 to 2.51	0 to 13.43	0 to 4.53	0.43 to 13.43	0 to 2.44	0 to 1.32
Number	20	50	36	14	20	20

the variables followed a normal distribution, the arithmetic means corresponding to each group were compared using the *t* test or the 1-way analysis of variance (ANOVA). When variables did not follow a normal distribution, a nonparametric test was used (Mann-Whitney *U* or ANOVA on ranks) to compare medians. Data from Groups 1 and 2 from Study 1 were compared and also compared with corresponding data from Groups C and D from Study 2.

Results

Nonoperated Eyes and ACS-Flap Eyes

Table 1 and Figure 2 present the WHO mean index values for the nonoperated corneas (Group A) and for the corneas that had surgery using the ACS (Group B), Hansatome (Group C), or M2 (Group D) microkeratomes. In Group A, the mean WHO index was 0.96 ± 0.68 (SD), which was significantly different from the corresponding values in Groups B, C, and D ($P<.001$). For the corneas with ACS-made flaps, the mean WHO index was 1.29 ± 2.03, which was significantly greater than for the Hansatome and M2 flaps ($P<.001$). However, a separate analysis of the reflectivity profile peak area in the 14 eyes with subclinical haze (5.54 ± 4.10) compared with that of the remaining 36 clear corneas (0.82 ± 0.85) displayed significant differences ($P<.001$).

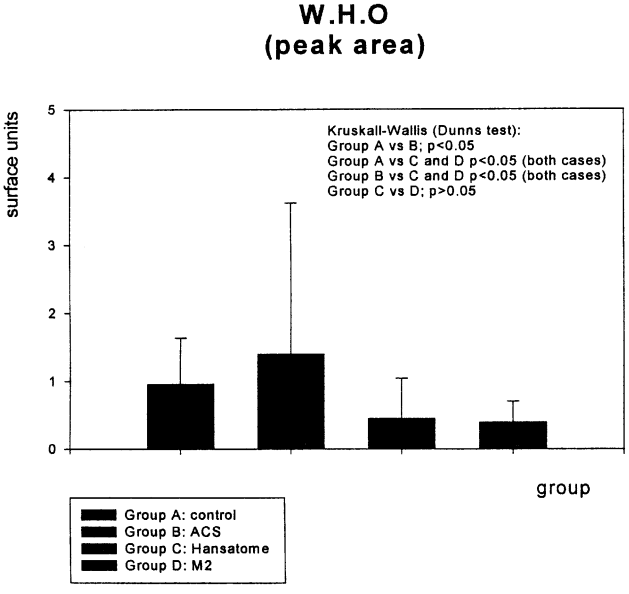

Figure 2. (Javaloy) Mean ± SD of the corneal WHO index (corneal opacity related with the wound-healing process) using the ACS, Hansatome, and M2 microkeratomes.

Table 2 exhibits preoperative spherical equivalent, preoperative pachymetry, flap thickness, differences between the desired and the actual flap thickness, and particle density (number/mm^2). Flaps made with the ACS microkeratome were significantly thinner than those made with the Hansatome or with the M2 ($P<.001$). The ACS also exhibited greater differences between the desired and the actual flap dimensions ($P<.001$).

The density of particles found at the interface was significantly lower in the eyes with ACS-made flaps ($P<.001$), which correlates with the smaller diameter of the ACS flaps compared with the Hansatome or M2 flaps. There were no cases with clinically significant haze (greater than +1), but a very slight subclinical lack of transparency (smaller than +1) was detected in 14 eyes with the ACS-made flaps (Figure 2).

There was no significant linear correlation between the depth of the cut and the confocal WHO value ($r = 0.10$). A scatterplot of the luminous reflectivity area in the anterior stroma vs. the flap thickness (Figure 3) suggests that not every thin flap creates subclinical haze. However, in all corneas that were not completely clear, the depth of the cut was <120 μm. Furthermore, only some of the corneas with ACS-created flap had subclinical haze. Figure 4 also illustrates the lack of correlation between particle density and the confocal WHO score ($r = 0.167$).

Hansatome-Flap and M2-Flap Eyes

In Study 2 (Hansatome vs. M2), flaps were consistently thicker in eyes in which the flap was made with the M2 microkeratome than with the Hansatome (Table 2). The difference between the arithmetic mean flap

Table 2. Spherical equivalent, flap thickness, particle density at the central interface, and desired minus actual flap thickness for the Hansatome, M2, and ACS microkeratomes: mean ± standard deviation (range).

	Preoperative Spherical Equivalent (D)	Preoperative Pachymetry (μm)	Flap Thickness (μm)	Particle Density (n/mm²)	Difference Desired vs. Actual Flap Thickness (μm)
Hansatome microkeratome	−5.3 ± 2.49 −1 to −9.5	554.08 ± 28.8	—	—	—
1st week	—	—	133.71 ± 20.38 102 to 165	169.58 ± 119.41 59 to 407	26.28 ± 20.38 −5 to 58
1st month	—	—	134.87 ± 24.88 98 to 190	144.30 ± 93.47 59 to 310	20.50 ± 30.70 −30 to 62
M2 microkeratome	−5.20 ± 2.53 −3.75 to −11	554.86 ± 32.7	— —	— —	— —
1st week	—	—	150.13 ± 20.42 109 to 189	143.52 ± 57.24 57 to 143	9.87 ± 20.42 −29 to 51
1st month	—	—	147.61 ± 15.439 119 to 184	148.00 ± 94.49 14 to 473	12.39 ± 15.44 −24 to 41
ACS microkeratome	−4.62 ± 2.47 −3.75 to 12	541.08 ± 57.4	102.01 ± 24.89 52 to 188	32.80 ± 48.73 0 to 310	57.98 ± 24.89 28 to 98

thickness produced by the Hansatome and the M2 was statistically significant at week 1 and month 1 ($P = .007$).

To estimate the predictability of the microkeratomes, the difference between the desired flap thickness (160 μm) and the thickness actually obtained with both microkeratomes was also analyzed. Differences were significantly higher with Hansatome-created flaps at week 1 ($P = .039$), and at month 1 ($P = .022$) (Table 2 and Figure 5).

The density of interface particles was not significantly different for the 2 microkeratomes ($P = .975$). The calculated mean WHO index was 0.44 ± 0.59 for the Hansatome surgeries and 0.39 ± 0.31 for the M2 surgeries, and the differences were not significant.

The mean size of flaps made with the Hansatome was significantly larger than those made with the M2 ($P<.001$) (Table 3). However, a comparison of the difference in absolute values of the real diameter and the desired diameter revealed no significant difference ($P = .35$). The mean length of the flap hinge was

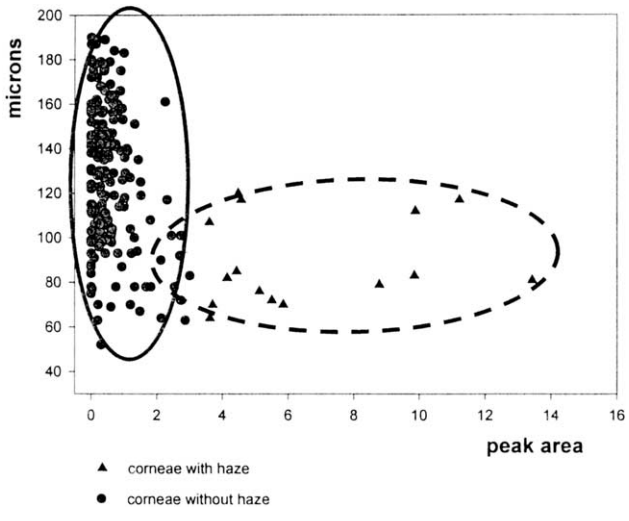

Figure 3. (Javaloy) Scatterplot illustrating the depth of the cut and the corresponding WHO index. Only some of the thinnest flaps (made with the ACS microkeratome in all cases) displayed subclinical haze (inside dashed line).

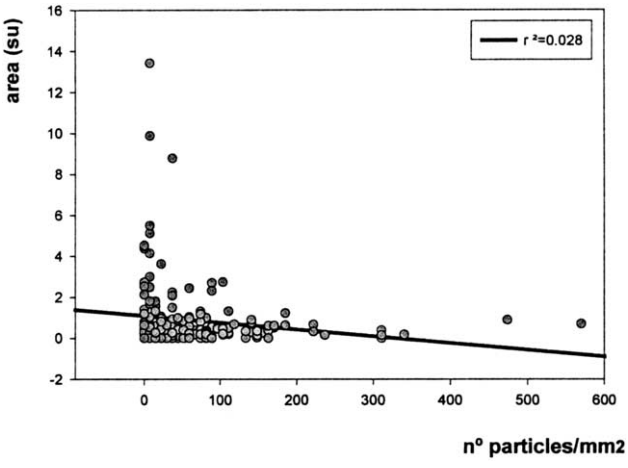

Figure 4. (Javaloy) Poor correlation between the WHO index and the density of the particles at the interface considering all cases.

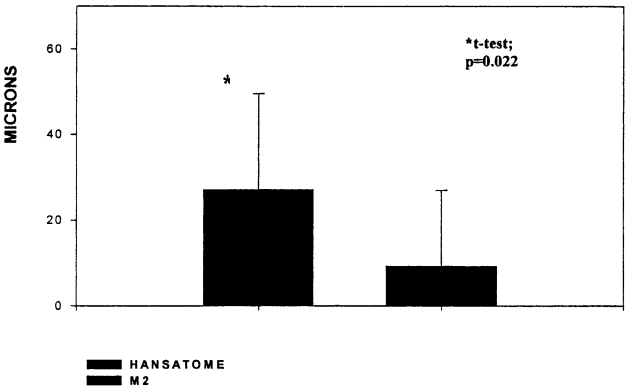

Figure 5. (Javaloy) Differences between the desired flap thickness and the actual obtained using both third-generation microkeratomes.

significantly larger with the Hansatome than with the M2 ($P<.001$). A comparison of the differences in absolute value of the actual obtained length of the hinge vs. the desired length also exhibited no significant difference ($P = .18$).

The mean microkeratome handling comfort and performance scores (surgeon's subjective questionnaire) were similar for the 2 microkeratomes ($P = .54$). However, the quality of the flap scores were significantly different and better with the M2 than with the Hansatome ($P = .04$) (Table 3).

Discussion

The cut made by the microkeratome is highly relevant to the final outcomes of LASIK surgery because it can induce the most severe complications of the procedure. Thus, clinical and experimental models that evaluate the quality of microkeratome technology make an important contribution to LASIK surgery.

As a direct, objective, and appraisable technique, confocal microscopy is an important tool in the development of quality models. Optical confocal microscopy has advantages over conventional optical microscopy because it does not cause "blurring of images out of focus" and makes it possible to obtain in vivo serial optical cuts. Confocal microscopy therefore obtains images of higher resolution than those obtained by conventional microscopy.[26,27]

The CMTF analysis is based on the observation that successive layers of the cornea generate different reflective intensities. A software program has been developed to analyze the light reflectivity at each point of the cornea. Since every point of the CTMF curve correlates directly with an image, it can be used to accurately calculate the distance between different corneal sublayers. This technique has been demonstrated to reliably measure corneal epithelial, stromal, and endothelial thickness.[24,28–30] Also, recent studies that used CMTF to measure flap thickness in eyes after LASIK surgery observed good predictability.[13,17] A detailed study in rabbits has validated CMTF as an accurate and precise technique for corneal sublayer pachymetry.[46] This study also presented the small influence of factors, such as radius of curvature (7.0 to 9.0), changes in target thickness (300 to 600 μm), thickness of the immersion fluid (0 to 300), and scan speed (20 to 80 μm/sec), in the accuracy of the technique.

In addition, CM permits quantification of the number of particles found at the interface and the degree of the opacity related to corneal wound healing. Furthermore, some authors have described the existence of a peak in CMTF curves, where area must correlate with the degree of corneal opacity.[24,29–31] The measurement of the reflected light intensity at each point of the *z*-axis during an epithelium to endothelium scan permits us to objectively quantify the extent of any moderate or even subclinical corneal haze. We have described corneal WHO index, to the area of the peak that appears at the CMTF profile in the anterior part of the corneal stroma (Figure 1).

The role of this peak in cut quality remains to be explored, but it is likely to be important. In fact, CMTF

Table 3. Surgeon scores for microkeratome handling comfort, appearance of the flap after the procedure, and dimensions of the flap and hinge: Mean ± standard deviation.

Microkeratome	Handling Comfort	Flap Quality	Flap Diameter (mm)	Hinge (mm)
Hansatome	9.00 ± 0.67 6.0 to 10.0	3.44 ± 0.53 3.0 to 4.0	9.80 ± 0.37 9.25 to 10.5	5.10 ± 0.45 5.7 to 4.25
M2	8.47 ± 1.46 6.0 to 10.0	4.0 4.0 to 4.0	9.30 ± 0.33 8.75 to 10.0	4.74 ± 0.32 5.25 to 4.5

analysis has never been used to evaluate the quality of microkeratome cuts, considering at the same time the degree of subclinical opacity at the anterior part of the corneal stroma, the density of particles found at the interface, and the flap thickness. Systematizing this technique should be a very useful tool for assessment in corneal refractive surgery.

Scanning electronic microscopy has been helpful for the experimental analysis of microkeratomes. Regarding the interface, cut quality has been studied from the point of view of blades, new or used blades,[18] and the smoothness and sharpness before and after the cuts.[18,22] The quality and mechanical features (system and cut speed) of different models of microkeratomes as they affect the quality of flap edges and the interface have been considered as well.[23]

Development of a technique capable of analyzing the cut quality in the cornea in vivo is needed in light of the great variety of microkeratomes on the market and the increasing use of LASIK surgery. Whereas CM up to now has been mostly an experimental exploratory technique, we have found it to have great clinical relevance. For us, CM was an invaluable method for studying the global quality of different microkeratomes, including parameters closely related to the accuracy of these devices, such as particle density, depth of the cut, and corneal opacity after surgery.

Corneal opacity after photorefractive surgery using CM has been objectively measured in previous studies,[24,29–31] but none has applied CMTF analysis to the systematic evaluation of LASIK surgery quality. Although the importance of the interface surface smoothness or the presence of particles in this virtual space in corneal transparency has not yet been well determined, it seems logical to have consequences in the healing process at this level.

Different methods have been used to evaluate the flap thickness: intraoperative substraction pachymetry,[19,20,32,34,35] optical coherence tomography,[33,36] and very high frequency ultrasound biomicroscopy.[37,38] Ultrasonic and optical coherence tomograph pachymetry achieve lower resolution power than CMTF analysis (12, 6, and 2.6 μm, respectively).[13] Several studies report important differences among the expected flap thickness that should be obtained with a model of microkeratome and the thickness actually obtained. For ACS microkeratome, flaps 20% to 30% thinner than expected for 130, 160, and 180 heads have been reported.[13,17,35] For Hansatome, similar results have been published.[19,20,34] Until now, there were no studies published reporting the predictability of flap thickness for M2 microkeratome.

Two parameters in our studies indicate that the M2 microkeratome is more accurate in flap thickness than the Hansatome and the ACS: a smaller standard deviation in the mean flap thickness and a smaller difference between the desired flap thickness and the thickness actually obtained. Since considerable differences between the intended cut depth and the actual have been revealed,[32–34] adequate assessment of this parameter in the evaluation of microkeratome global quality is vital. In addition, significant differences in flap thickness have been proved, using only 1[19,39] or different units of the same microkeratome model.[40] Thus, we consider it clinically important to study each unit in use in our center by means of CMTF analysis.

The lack of significant differences between the Hansatome and M2 microkeratomes for desired and actual surface dimensions of the flap indicates a similar and adequate reliability of both instruments at this biometric level. Likewise, similar values for both microkeratomes for the corneal WHO index suggest no important differences in the wound-healing process at the interface. We suggest that both microkeratomes make their cut deeper than the layer just next to Bowman's membrane, where keratocytes are numerous. Furthermore, if we have few activated keratocytes and an interface deep and far from the epithelium, as well as from the vessels, tears, and nerves that have inflammatory components, clinical or subclinical haze is likely to be rare. We agree with previous reports that the integrity of the most anterior keratocyte layer is necessary for controlling keratocyte activation and haze formation.[17,30,41]

Our results suggest that a cut made deeper than 120 μm does not induce haze by itself. This should explain the differences found in the confocal WHO scores between the corneas cut with the ACS microkeratome and the Hansatome and M2 microkeratomes because the ACS created thinner flaps. The lack of linear correlation between flap thickness and subclinical opacity can perhaps be explained by different corneas having different capability to form haze. A great variety of circumstances, such as the density or availability of activation of the anterior keratocyte population, the amount and nature of the released cytokines,[42,43] age of

patients,[44] thermal effect of the laser,[45] or other unknown conditions, could provide a different capability of response in every case.

In operated eyes, it has been proved that keratocyte density remains low at the immediate anterior and posterior interfaces during a period of time superior to 12 months.[47] Apoptosis possibly related with alterations in corneal innervation induced by LASIK seems to be responsible for this depopulation.[41,48–50] From our point of view, the low anterior keratocyte density and subbasal nervous plexus alterations in operated eyes not presenting subclinical haze might be responsible for the lower optical reflectivity (WHO index) with respect to nonoperated (control) eyes.

This study suggests that the presence of normal amounts of metallic or organic particles at the interface does not affect the healing process in terms of secondary corneal opacity.[41] The lower density of particles found in interfaces when the ACS was used could be a result of the smaller surface dimension of ACS flaps. It seems quite logical that the capability of a constant (automated) irrigation flow to clean under a small flap was greater than under a larger flap. Another possible reason to explain this fact could be a more comfortable maneuver for surgeons used to irrigate flaps with nasal hinge.

Although the handling comfort during the cut was very similar with both microkeratomes, the apparent quality of the flap created by the M2 microkeratome was better than that made by the Hansatome. This opinion about apparent quality of the flap coincides with the objective findings of this study.

Conclusion

The TSCM provides valuable information for evaluating the quality of cut made by a microkeratome. The model presented here using the confocal microscope (confocal pachymetry, density of particles, and WHO index) appears as a useful tool to evaluate different models of microkeratomes. The M2 microkeratome consistently made thicker cuts and exhibited better predictability than the Hansatome or the ACS. However, the quantity of particles and the healing process of the cut interface were very similar with both instruments. The depth of the cut, but not the density of the particles at the interface, seems to influence corneal transparency after LASIK surgery. Overall, the predictability of flap thickness and the apparent quality of the cut made by the Moria M2 microkeratome are better than those obtained with the Hansatome or the ACS.

References

1. Sugar A, Rapuano CJ, Culbertson WW, Huang D, et al. Laser in situ keratomileusis for myopia and astigmatism: safety and efficacy. (Opthalmic Technologies Assessment) A report by the American Academy of Ophthalmology. Ophthalmology 2002; 109:175–187
2. Walker MB, Wilson SE. Lower intraoperative flap complication rate with the Hansatome microkeratome compared to the Automated Corneal Shaper. J Refract Surg 2000; 16:79–82
3. Jacobs JM, Taravella MJ. Incidence of intraoperative flap complications in laser in situ keratomileusis. J Cataract Refract Surg 2002; 28:23–28
4. Knorz MC. Flap and interface complications in LASIK. Curr Opin Ophthalmol 2002; 13:242–245
5. Yildirim R, Devranoglu K, Ozdamar A, et al. Flap complications in our learning curve of laser in situ keratomileusis using the Hansatome microkeratome. Eur J Ophthalmol 2001; 11:328–332
6. Kuo IC, Ou R, Hwang DG. Flap haze after epithelial debridement and flap hydration for treatment of post-laser in situ keratomileusis striae. Cornea 2001; 20: 339–341
7. Pallikaris IG, Kymionis GD, Astyrakakis NI. Corneal ectasia induced by laser in situ keratomileusis. J Cataract Refract Surg 2001; 27:1796–1802
8. Carlson KH, Carpel EF. Epithelial folds following slippage of LASIK flap. Ophthalmic Surg Lasers 2000; 31: 435–437
9. Pallikaris IG, Katsanevaki VJ, Panagopoulou SI. Laser in situ keratomileusis intraoperative complications using one type of microkeratome. Ophthalmology 2002; 109: 57–63
10. Buratto L, Brint S. LASIK with a nasal hinge using the ACS microkeratome. In: Buratto L, Brint S, eds, LASIK; Surgical Techniques and Complications, 2nd ed. Thorofare, NJ, Slack, 2000; 103–129
11. Hamill MB, Kohnen T. Scanning electron microscopic evaluation of the surface characteristics of 4 microkeratome systems in human corneas. J Cataract Refract Surg 2002; 28:328–336
12. Shemesh G, Dotan G, Lipshitz I. Predictability of corneal flap thickness in laser in situ keratomileusis using three different microkeratomes. J Refract Surg 2002; 18: S347–S341
13. Gokmen F, Jester JV, Petroll WM, et al. In vivo confocal microscopy through-focusing to measure corneal flap thickness after laser in situ keratomileusis. J Cataract Refract Surg 2002; 28:962–970

14. Tole DM, McCarty DJ, Couper T, Taylor HR. Comparison of laser in situ keratomileusis and photorefractive keratectomy for the correction of myopia of −6.00 diopters or less; the Melbourne Excimer Laser Group. J Refract Surg 2001; 17:46–54
15. Lyle WA, Jin GJC. Results of flap repositioning after laser in situ keratomileusis. J Cataract Refract Surg 2000; 26:1451–1457
16. Booranapong W, Malathum P, Slade SG. Anatomic factors affecting microkeratome placement in laser in situ keratomileusis. J Cataract Refract Surg 2000; 26:1319–1325
17. Vesaluoma M, Pérez Santonja J, Petroll M, et al. Corneal stromal changes induced by myopic LASIK. Invest Ophthalmol Vis Sci 2000; 41:369–376; erratum, 2027
18. Behrens A, Langenbucher A, Kus MM, et al. Experimental evaluation of two current-generation automated microkeratomes: the Hansatome and the Supratome. Am J Ophthalmol 2000; 129:59–67
19. Yildirim R, Aras C, Ozdamar A, et al. Reproducibility of corneal flap thickness in laser in situ keratomileusis using the Hansatome microkeratome. J Cataract Refract Surg 2000; 26:1729–1732
20. Gailitis RP, Lagzdins M. Factors that affect corneal flap thickness with the Hansatome microkeratome. J Refract Surg 2002; 18:439–443
21. Spadea L, Cerrone L, Necozione S, Balestrazzi E. Flap measurements with the Hansatome microkeratome. J Refract Surg 2002; 18:149–154
22. Wilhelm F, Giesmann T, Hanschke R, Duncker G. Schnittkanten nach lamellärer Keratotomie mit verschiedenen Mikrokeratomen. Klin Monatsbl Augenheilkd 1998; 213:293–300
23. Wilhelm FW, Giessmann T, Hanschke R, et al. Cut edges and surface characteristics produced by different microkeratomes. J Refract Surg 2000; 16:690–700
24. Møller-Pedersen T, Cavanagh D, Petroll M, Jester JV. Stromal wound healing explains refractive instability and haze development after photorefractive keratectomy; a 1-year confocal microscopic study. Ophthalmology 2000; 107:1235–1245
25. Declaration of Helsinki. Adopted by the 18th World Medical Assembly, Helsinki, Finland, June 1964
26. Petráň M, Hadravskŷ M, Egger MD, Galambos R. Tandem-scanning reflected-light microscope. J Opt Soc Am 1968; 58:661–664
27. Boyde A. Applications of tandem scanning reflected light microscopy and three-dimensional imaging. Ann NY Acad Sci 1986; 483:428–439
28. Kauffman T, Bodanowitz S, Hesse L, Kroll P. Corneal reinnervation after photorefractive keratectomy and laser in situ keratomileusis: an in vivo study with a confocal videomicroscope. Ger J Ophthalmol 1997; 5:508–512
29. Li HF, Petroll WM, Møller-Pedersen T. Epithelial and corneal thickness measurements by in vivo confocal microscopy through focusing (CMTF). Curr Eye Res 1997; 16:214–221
30. Møller-Pedersen T, Li HF, Petroll WM, et al. Confocal microscopic characterization of wound repair after photorefractive keratectomy. Invest Ophthalmol Vis Sci 1998; 39:487–501
31. Møller-Pedersen T, Vogel M, Li HF, et al. Quantification of stromal thinning, epithelial thickness, and corneal haze after photorefractive keratectomy using in vivo confocal microscopy. Ophthalmology 1997; 104:360–368
32. Durairaj VD, Balentine J, Kouyoumdjian G, et al. The predictability of corneal flap thickness and tissue laser ablation in laser in situ keratomileusis. Ophthalmology 2000; 107:2140–2143
33. Genth U, Mrochen M, Walti R, et al. Optical low coherence reflectometry for noncontact measurements of flap thickness during laser in situ keratomileusis. Ophthalmology 2002; 109:973–978
34. Maldonado MJ, Ruiz-Oblitas L, Munuera JM, et al. Optical coherence tomography evaluation of the corneal cap and stromal bed features after laser in situ keratomileusis for high myopia and astigmatism. Ophthalmology 2000; 107:81–87; discussion by DR Hardten, 88
35. Pérez-Santonja JJ, Bellot JL, Claramonte P, et al. Laser in situ keratomileusis to correct high myopia. J Cataract Refract Surg 1997; 23:372–385
36. Feng Y, Varikooty J, Simpson TL. Diurnal variation of corneal and corneal epithelial thickness measured using optical coherence tomography. Cornea 2001; 20:480–483
37. Reinstein DZ, Silverman RH, Sutton HFS, Coleman DJ. Very high-frequency ultrasound corneal analysis identifies anatomic correlates of optical complications of lamellar refractive surgery; anatomic diagnosis in lamellar surgery. Ophthalmology 1999; 106:474–482
38. Reinstein DZ, Silverman RH, Raevsky T, et al. Arc-scanning very high-frequency digital ultrasound for 3D pachymetric mapping of the corneal epithelium and stroma in laser in situ keratomileusis. J Refract Surg 2000; 16:414–430
39. Yi W-M, Joo C-K. Corneal flap thickness in laser in situ keratomileusis using an SCMD manual microkeratome. J Cataract Refract Surg 1999; 25:1087–1092
40. Liu K-Y, Lam DSC. Direct measurement of microkeratome gap width by electron microscopy. J Cataract Refract Surg 2001; 27:924–927
41. Pisella PJ, Auzerie O, Bokobza Y, et al. Evaluation of corneal stromal changes in vivo after laser in situ keratomileusis with confocal microscopy. Ophthalmology 2001; 108:1744–1750
42. Wilson SE, He Y-G, Weng J, et al. Epithelial injury induces keratocyte apoptosis: hypothesized role for the interleukin-1 system in the modulation of corneal tissue

organization and wound healing. Exp Eye Res 1996; 62:325–337
43. Møller-Pedersen T, Cavanagh HD, Petroll WM, Jester JV. Neutralizing antibody TGFβ modulates stromal fibrosis but not regression of photoablative effect following PRK. Curr Eye Res 1998; 17:736–747
44. Berlau J, Becker H-H, Stave J, et al. Depth and age-dependent distribution of keratocytes in healthy human corneas; a study using scanning-slit confocal microscopy in vivo. J Cataract Refract Surg 2002; 28:611–616
45. Maldonado-Codina C, Morgan PB, Efron N. Thermal consequences of photorefractive keratectomy. Cornea 2001; 20:509–515
46. Ivarsen A, Stultiens BAT, Møller-Pedersen T. Validation of confocal microscopy through focusing for corneal sublayer pachymetry. Cornea 2002; 21:700–704
47. Mitooka K, Ramirez M, Maguire LJ, et al. Keratocyte density of central human cornea after laser in situ keratomileusis. Am J Ophthalmol 2002; 133:307–314
48. Helena MC, Baerveldt F, Kim W-J, Wilson SE. Keratocyte apoptosis after corneal surgery. Invest Ophthalmol Vis Sci 1998; 39:276–283
49. Wilson SE, Kim W-J. Keratocyte apoptosis: implications on corneal wound healing, tissue organization, and disease. Invest Ophthalmol Vis Sci 1998; 39:220–226
50. Wilson SE. Laser in situ keratomileusis-induced (presumed) neurotrophic epitheliopathy. Ophthalmology 2001; 108:1082–1087

From the Department of Cornea and Refractive Surgery (Javaloy, Vidal, Alió), Instituto Oftalmológico de Alicante, Miguel Hernández University, the Instituto Oftalmológico de Alicante (Quinto), Alicante, and the Instituto Gallego de Oftalmología (de Rojas), Universidad de Santiago de Compostela, Spain.

The authors declare no proprietary or financial interest about any of the products used in the study.

This study was supported in part by a grant from the Spanish Ministry of Science and Technology, Red Temática de Investigación en Oftalmologia, Subproyecto de Cirugia Refractiva y Calidad Visual (C03/13).